

MOLECULAR ORBITAL ANALYSIS OF THE BONDING IN PENTA- AND HEPTA-NUCLEAR GOLD TERTIARY PHOSPHINE CLUSTERS

DAVID G. EVANS and D. MICHAEL P. MINGOS*

Inorganic Chemistry Laboratory, University of Oxford, South Parks Road, Oxford, OX1 3QR (Great Britain)

(Received May 23rd, 1985)

Summary

The structural features of gold tertiary phosphine clusters $Au_n(PR_3)_n^{x+}$ ($n = 5$ and 7) have been analysed using Extended Hückel calculations. The most favoured metal geometry and ligand conformation is found to be that which leads to the maximum hybridisation of Au $6s$ character into the cluster bonding molecular orbitals. The conclusions derived have been utilised to predict the existence of a number of some homo- and hetero-nuclear clusters containing gold.

The synthesis and reactions of gold phosphine clusters is a topic of considerable current interest [1,2] and has been recently reviewed [3]. Our attempts to understand the electronic structures of such clusters date from 1976 [4] with the prediction of the geometry and stoichiometry of the first example of a centred icosahedral metal cluster compound which was subsequently prepared in our laboratories [5]. In a previous paper in this series [6] we have demonstrated how the structures of gold cluster compounds of the type $Au_n(PR_3)_n^{x+}$ depend crucially on the nature of the frontier orbitals of the constituent $Au(PR_3)$ fragments which are illustrated on the left hand side of Fig. 1. The molecular orbital model provided a framework for a discussion of the bonding in some tetra- and hexanuclear gold clusters [6] and the subsequent extension of this analysis to high nuclearity $Au_n(PR_3)_{n-1}^{x+}$ ($n = 8-13$) clusters which contain a central interstitial gold atom [7].

In this paper, which was stimulated by the recent synthesis and structural characterisation [8] of the pentagonal bipyramidal cluster $Au_7(PPh_3)_7^+$, we report a molecular orbital analysis of the bonding in a range of penta- and hepta-nuclear gold clusters. We make use of elementary symmetry and perturbation theory arguments supported by Extended Hückel calculations with the parameters given in the Appendix. The analysis may be most conveniently expressed using the nomenclature of Tensor Surface Harmonic Theory (TSH) used by Stone [9,10] to rationa-

lise the bonding in borane clusters. The way in which this applies to $[\text{Au}(\text{PR}_3)]_n$ clusters will now be briefly summarised.

Consider first n B–H fragments which are arranged on the surface of a sphere. The n fragment radial $hy(s-z)$ orbitals give rise to S^σ , P^σ , d^σ etc. combinations up to a total of n . For $n \leq 5$ all except the S^σ are antibonding whilst the P^σ become approximately non-bonding ($n=6$) and then progressively more bonding with increasing nuclearity. The $2n$ fragment tangential (p_x and p_y) orbitals give rise to n bonding (P^π , D^π , F^π etc.) and n antibonding (P^σ , D^π , F^π , etc.) combinations. For any symmetry lower than the spherical case implicit in Stone's analysis it is necessary to take into account mixing between σ and π levels. Mixing between P^σ and P^π generates one bonding P set of predominantly P^σ character [9] and one antibonding P set of predominantly P^π character. Mixing between D^σ and D^π (which is less on the grounds of their greater energy separation) has the same effect. Thus in a *closo*-deltahedron there are a total of $(n+1)$ bonding skeletal MO's which are all occupied.

The calculated molecular orbital diagrams for the set of $\text{Au}_n(\text{PH}_3)_n$ clusters, $n=3-7$, are illustrated in Fig. 1 [6]. These calculations confirm the presence of the one strongly bonding S^σ orbital, but indicate that the P^σ/π and D^π sets, although metal-metal bonding, are generally too high lying to be occupied as a consequence of the large $s-p$ separation and relatively low Au $6p-6p$ overlap integrals. In clusters of cubic symmetry such as the octahedral $\text{Au}_6(\text{PR}_3)_6$ species the three components of the P^σ/π set are degenerate. On going to ellipsoidal clusters of general D_{nh} symmetry the $P_{x,y}^\sigma/\pi$ and P_z^σ/π orbitals are no longer degenerate. In the trigonal bipyramidal case the P_z^σ/π orbital acquires a greater amount of Au $6s$ character and is stabilised relative to the other two. In the case of the pentagonal bipyramidal cluster it is the $P_{x,y}^\sigma/\pi$ set which acquires the greater amount of Au $6s$ character, suggesting that its occupation may become favourable. The expected number of skeletal bonding electron pairs is therefore considerably less than $(n+1)$ and in fact varies between one ($n=3$ and 4) up to a possible maximum of four ($n>7$).

In practice it is observed that when n is >7 the interstitial cavity in the cluster is sufficiently large to accommodate a central gold atom. Such clusters adopt either spherical topologies where all four orbitals (S^σ and three P^σ/π) are stabilised by interaction with the s and p orbitals of the central gold atom or toroidal clusters where the S^σ and $P_{x,y}^\sigma/\pi$ orbitals are stabilised in this way but the cluster P_z^σ/π orbital remains unoccupied [11].

It follows from this simple molecular orbital analysis that the cluster metal-metal bonding interactions are maximised for polyhedra with triangular faces because these generate the largest number of next-neighbour interactions between the $hy(s-z)$ orbitals of the individual $\text{Au}(\text{PH}_3)$ fragments, leading to maximum stabilisation of the S^σ orbital. As the nuclearity rises the stability of this orbital increases and it is tempting to speculate on the existence of the series of clusters $\text{Au}_n(\text{PR}_3)_n^{x-}$ ($x=n-2$), where this orbital alone is occupied. The presence of only a single multicentre bonding molecular orbital in each of these clusters however carries with it the implication (confirmed by the Mulliken overlap population analyses reproduced in Fig. 1) of a diminution of gold-gold bonding with increased nuclearity. This suggests that the larger members of this series at least are unlikely to be stable, although isoelectronic species with bridging ligands might be capable of isolation.

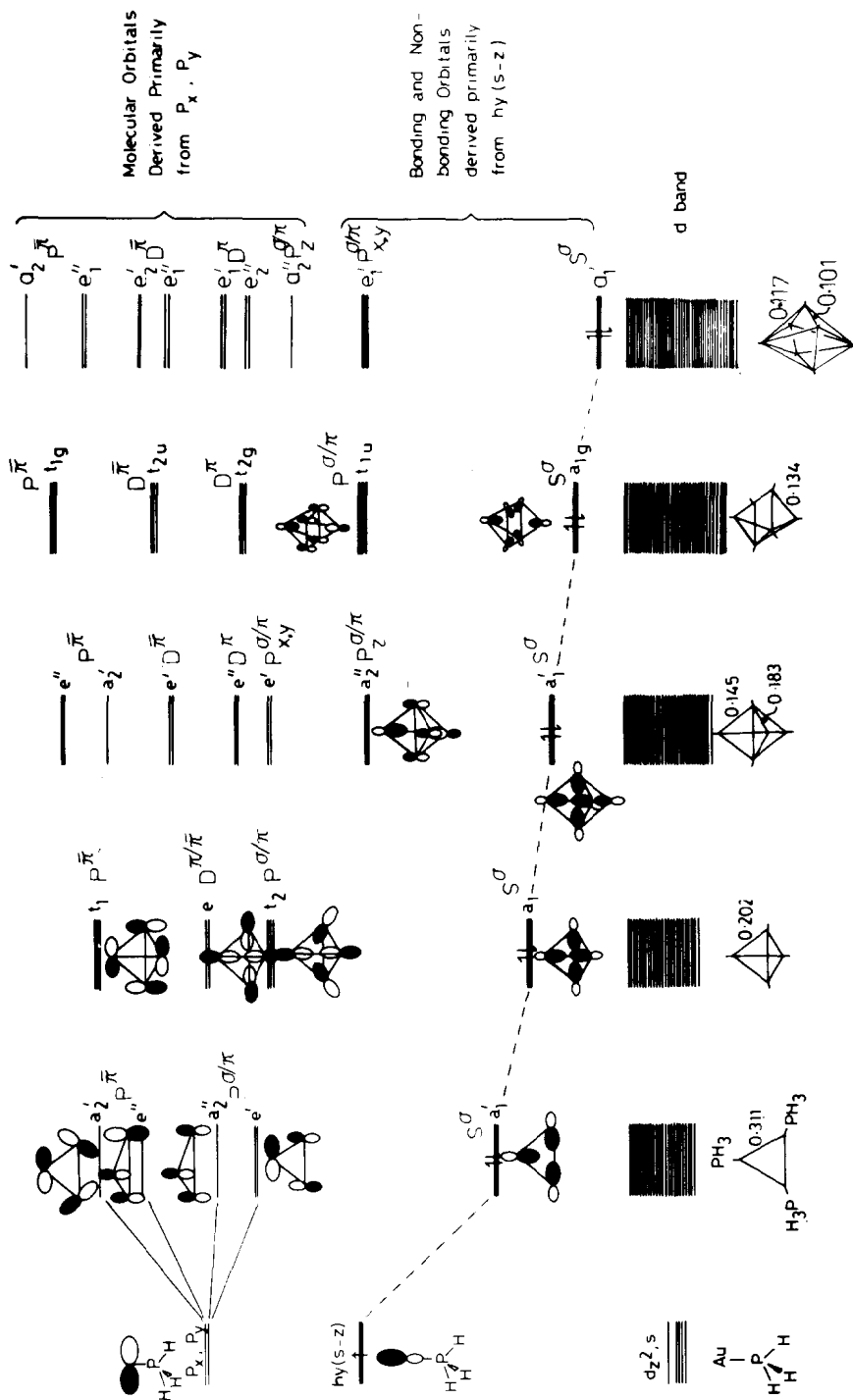


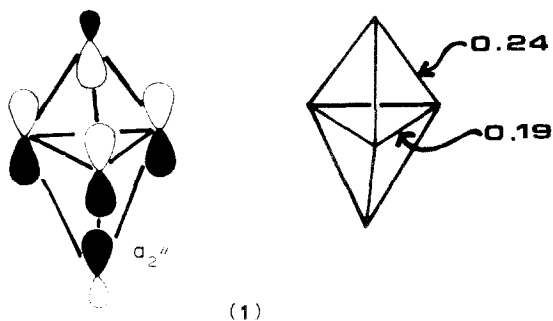
Fig. 1. The molecular orbitals of the deltahedral gold cluster $Au_n(PR_3)_n^{x+}$ ($x = n - 2$) as derived from the frontier orbitals of the $Au(PH_3)_3$ fragment, labelled in the notation of Tensor Surface Harmonic Theory. The computed overlap populations for these ions are given at the bottom of the Figure. In general occupation of only those MOs derived primarily from the fragment $h\nu(s-z)$ orbitals is feasible on energetic grounds.

The role of such bridging ligands has been discussed previously [6].

We will now analyse the bonding in some penta- and hepta-nuclear gold clusters containing $\text{Au}(\text{PR}_3)$ fragments in order to establish how their structures are related to the simple MO ideas presented above and in Fig. 1. We will also attempt to use the structural and bonding patterns derived to speculate on the existence of some as yet unknown cluster compounds.

Pentanuclear cluster compounds

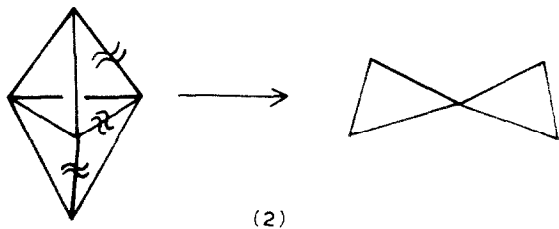
In the trigonal bipyramidal $\text{Au}_5(\text{PR}_3)_5$ cluster (see Fig. 1) there are expected to be two occupied skeletal MOs: a_1 (S^σ) and a_2'' (P^σ/π_z) with the other component of the P^σ/π set (e') having a much smaller P^σ contribution and being too weakly stabilised for occupation. This gives rise to the stoichiometry $\text{Au}_5(\text{PR}_3)_5^+$, with 64 electrons. The a_2'' orbital is σ -bonding between axial and equatorial atoms and π -bonding between the equatorial atoms, as shown in **1** so that the former six bonds are expected to be stronger and shorter. This is reflected in the computed Mulliken overlap populations for $\text{Au}_5(\text{PH}_3)_5^+$ also given in **1**.



The computed overlap populations suggest that such a cluster is potentially stable, although to date its synthesis has not been achieved.

An alternative more open geometry for the $\text{Au}_5(\text{PR}_3)_5^+$ cluster is the so-called bow-tie structure which consists of two triangles sharing a common vertex. This geometry has been reported for $\text{Os}_5(\text{CO})_{10}$ [12] and $\text{Fe}_4\text{M}(\text{CO})_{16}^{2+}$, ($\text{M} = \text{Pd}, \text{Pt}$) [13]. The bonding in such species has been discussed by us elsewhere [14].

The bow-tie geometry may be formally derived from the trigonal bipyramidal cluster by the breaking of one equatorial and two axial bonds as illustrated in **2**.



The effect of such a rearrangement on the frontier orbitals of the trigonal bipyramidal $\text{Au}_5(\text{PH}_3)_5^+$ cluster is illustrated in Fig. 2. The a_2'' orbital is strongly stabilised because more s character is introduced and the resulting b_1 orbital in the bow-tie geometry has a greater amount of σ -bonding character. The $a_1'(S^\sigma)$ orbital is

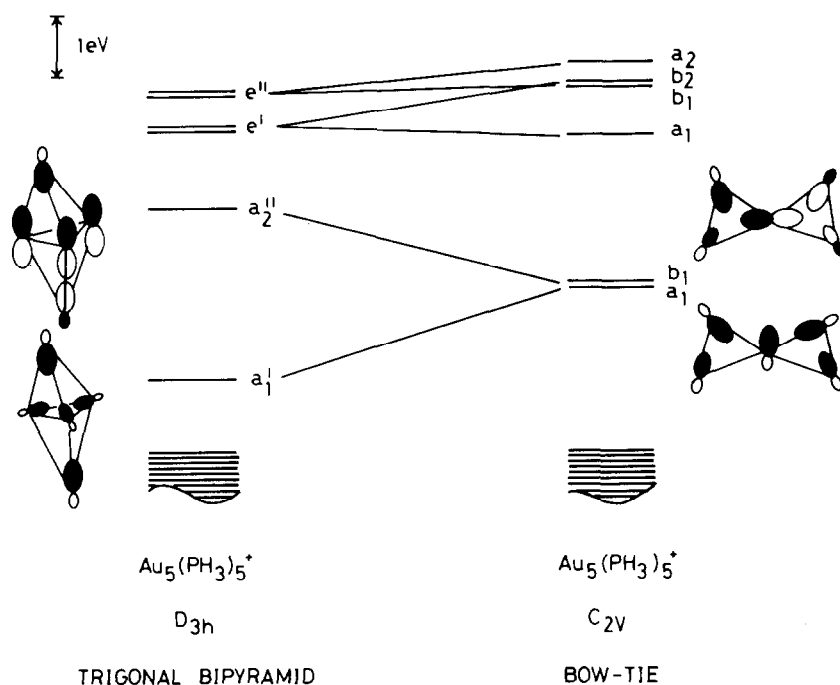
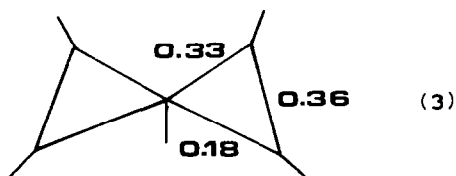


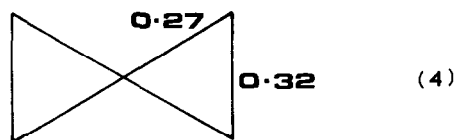
Fig. 2. The effect on the cluster bonding orbitals of $\text{Au}_5(\text{PH}_3)_5^+$ of a rearrangement from trigonal bipyramidal to a bow-tie geometry. The destabilisation of a_1' exceeds the stabilisation of a_2'' so that overall the trigonal bipyramidal is more stable.

strongly destabilised however because the overlap between the sp hybrid orbitals of the $\text{Au}(\text{PH}_3)$ fragments is less effective in the lower symmetry planar geometry. The calculations suggest that overall the bow-tie cluster is 0.6 eV less stable than the trigonal bipyramidal geometry.

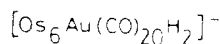
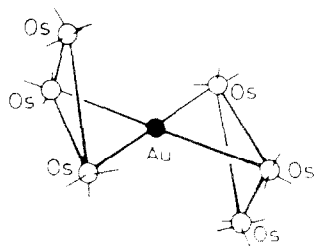
The bonding requirements of the central $\text{Au}(\text{PH}_3)$ fragment lead to a marked asymmetry in the computed Au–Au overlap populations as shown in 3.



This asymmetry is primarily a consequence of the nature of the a_1 cluster orbital which is less strongly bonding along two edges than the other four. Replacement of the central $\text{Au}(\text{PH}_3)^+$ fragment by Au leads to the more symmetrical distribution of overlap populations reproduced in 4.



Such a substitution is also favourable on steric grounds and taken together these factors suggest that the most likely stoichiometry for a pentanuclear cluster with the bow-tie geometry is $\text{Au}_5(\text{PR}_3)_4^+$. In such a cluster there are two skeletal electron pairs which in localised orbital terms can be considered as two three-centre two-electron bonds, one for each triangle. Although such a cluster has not yet been synthesised two related structures have been reported. Thus $\text{Fe}_3\text{M}(\text{CO})_{16}^{2-}$ ($\text{M} = \text{Pd}, \text{Pt}$) has the bow-tie geometry as mentioned above [14] in which the central metal atom is not coordinated to any ligands. The structure of the cluster $[\text{Os}_6\text{Au}(\text{CO})_{20}\text{H}_2]^-$ shown in **5** [15], can be considered to be derived from an Os_4Au bow-tie in which the Os-Os edge of each triangle has been bridged by an $\text{Os}(\text{CO})_4$ fragment.



(5)

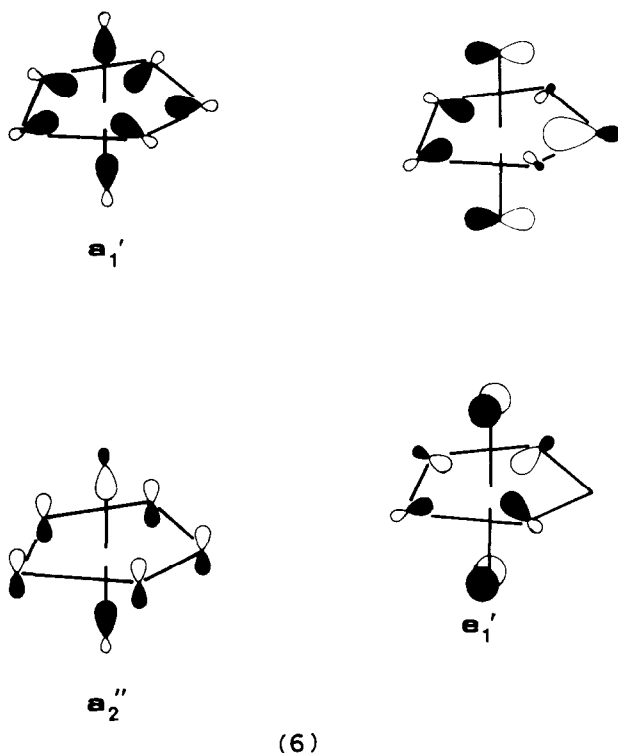
The central gold atom is coordinated to four metal atoms and no other ligands as suggested for $\text{Au}_5(\text{PR}_3)_4^+$ above. In **5** the bonding can also be described in terms of a pair of three-centre two-electron bonds within the Os_2Au triangles.

A number of heterometallic pentanuclear clusters containing gold have been structurally characterised [3]. The bonding in such clusters has been rationalised in terms of the ability of the $\text{Au}(\text{PR}_3)$ fragment to cap triangular faces of an existing cluster [3] and will not be discussed further in this paper.

Heptanuclear cluster compounds

The MO energy level diagram for a pentagonal bipyramidal $\text{Au}_7(\text{PH}_3)_7$ cluster illustrated in Fig. 1 indicates that of the eight skeletal bonding MOs expected for such a *closo*-deltahedron, four ($D^\pi = e_2'' + e_1'$) are too high lying to be occupied, being purely Au 6*p* in character. Of the three orbitals in the P^σ/P^π set, one (a_2'') is derived from an admixture of antibonding P_2^σ and bonding P^π and has Au 6*s* character on the axial atoms only whilst the e_1' set derived from bonding $P_{3,7}^\sigma$ and bonding P^π levels and has Au 6*s* character on the five equatorial atoms. There is thus an appreciable separation between the a_2'' and e_1' levels suggesting that only the latter is likely to be occupied together with the a_1' (S^σ) orbital, giving the stoichiometry $\text{Au}_7(\text{PH}_3)_7^+$. Furthermore, as shown in **6**, both a_1' and e_1' are bonding between the axial atoms whilst the a_2'' is antibonding.

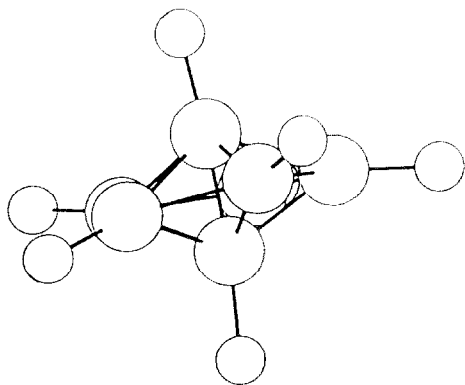
Thus occupation of a_1' and e_1' alone might be expected to favour a compression along the C_5 axis.



The cluster $\text{Au}_7(\text{PPh}_3)_7^+$ has recently been reported [8] and does have a distorted pentagonal bipyramidal geometry as illustrated in 7. Extended Hückel calculations which we have performed on $\text{Au}_7(\text{PH}_3)_7^+$ show that the potential energy surface associated with compression along the C_5 axis from an idealised pentagonal bipyramidal structure to a close approximation to the observed structure is in fact very soft, because the gain in bonding character across the *trans*-axial atoms is offset by the loss in bonding character within the equatorial plane.

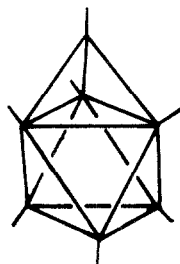
The energy level ordering for $\text{Au}_7(\text{PH}_3)_7^+$ given in Fig. 1 is in agreement with that deduced by Van der Velden et al. [8] on the basis of simple Hückel calculations involving only Au $6s$ - $6s$ overlaps on neighbouring atoms. In a recent paper Van der Velden and Stadnik [16] have related the electronic structure of $\text{Au}_7(\text{PH}_3)_7^+$ to the observed ^{197}Au Mössbauer spectral parameters of $\text{Au}_7(\text{PPh}_3)_7^+$.

Addition of two electrons would favour the formation of a regular or elongated pentagonal bipyramid because of the *trans*-axial antibonding character of the a_2'' orbital. The presence of four skeletal bonding MOs (of essentially S^σ and P^σ character) in such a case is directly analogous to the case of closed polyhedral Au_x clusters ($x = 8$ - 13) analysed elsewhere by Mingos [11]. In such cases these orbitals are stabilised by the presence of a central gold atom, utilising its $6s$ and $6p$ orbitals. Although the cavity in an Au_7 cluster is presumably too small to accommodate a gold atom it is tempting to speculate that a species such as $\text{Au}_7(\text{PR}_3)_7\text{C}^{3+}$ might be capable of isolation. If a non-centred cluster were to exist it would be most unlikely to be $\text{Au}_7(\text{PR}_3)_7^-$ by virtue of its charge and perhaps $\text{Au}_6\text{Hg}(\text{PR}_3)_7$ or $\text{Au}_5\text{Hg}_2(\text{PR}_3)_7^+$ are more likely species.



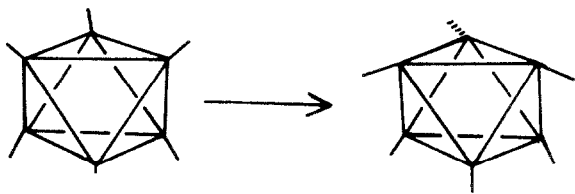
(7)

The ability of $\text{Au}(\text{PR}_3)$ to cap a triangular face of a cluster discussed elsewhere [3] suggest that the monocapped octahedron is an alternative structure for a heptanuclear gold cluster. The MO interaction diagram for the formation of the capped octahedral cluster **8** is illustrated in Fig. 3.



(8)

The $a_{1g}(S^o)$ orbital of the octahedron does not interact effectively with the capping group by virtue of its inward hybridisation and instead the frontier orbitals of the latter interact with the components of the $t_{1u}(P^o/P^o)$ set. The $h_1(s-z)$ orbital of the $\text{Au}(\text{PH}_3)^+$ fragment generates the strongly bonding $2a_1$ orbital whilst the tangential $6p$ orbitals give rise to the much more weakly bonding $1e$ set. Occupation of $1a_1$ and $2a_1$ alone leads to the stoichiometry $\text{Au}_7(\text{PR}_3)_2^{3+}$ whilst additional occupation of the $1e$ set gives $\text{Au}_7(\text{PR}_3)_7^-$. A lowering of the symmetry of the $\text{Au}_6(\text{PH}_3)_6$ cluster to C_{3v} , by the distortion of the phosphine ligands shown in **9** raises the degeneracy of the t_{1u} set as illustrated in Fig. 3.



(9)

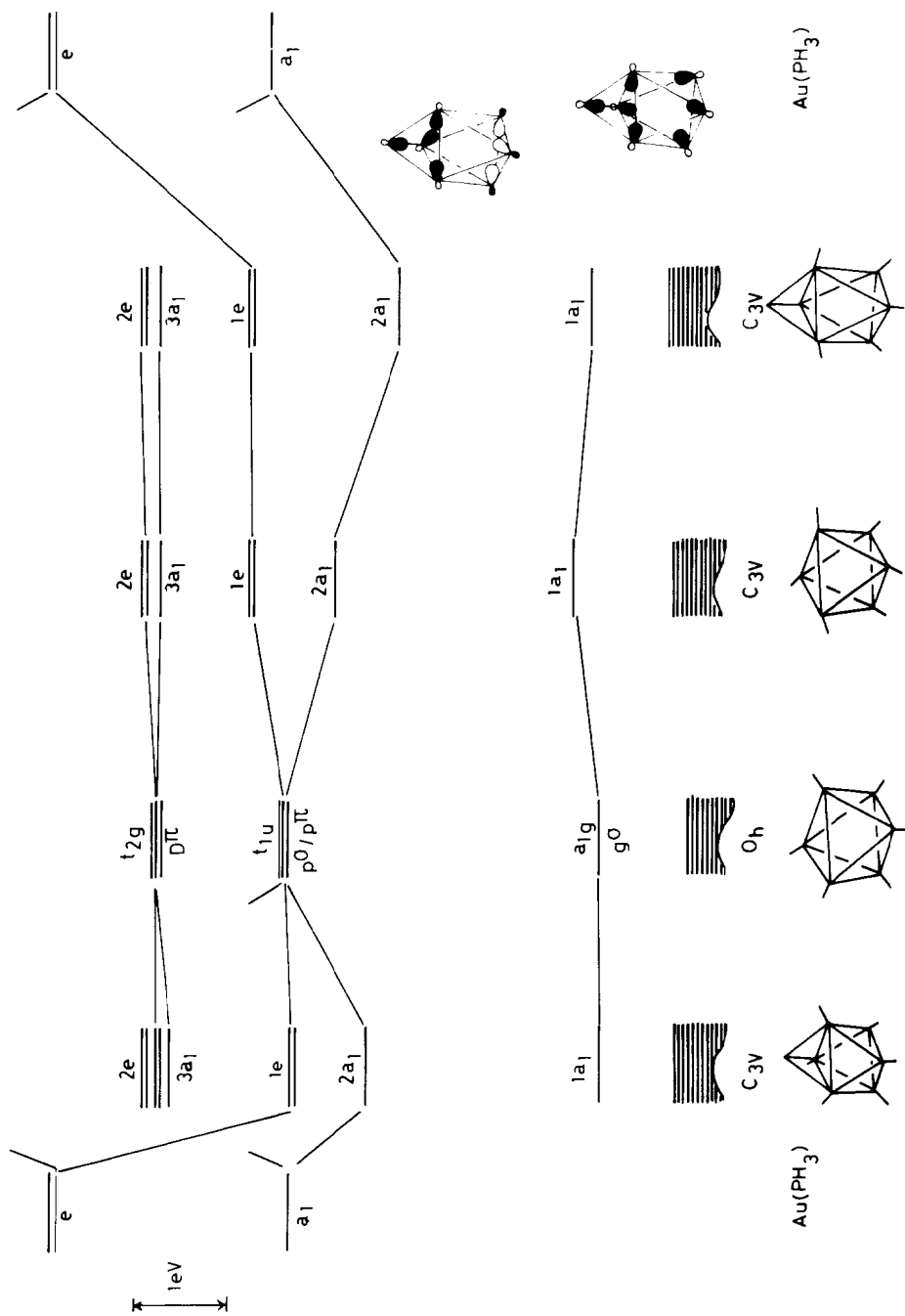
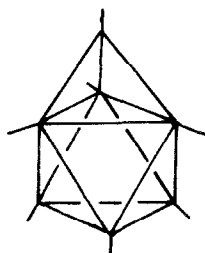


Fig. 3. The MO interaction diagram for the capping of octahedral $\text{Au}_6(\text{PH}_3)_6$ clusters with alternative ligand geometries by an $\text{Au}(\text{PH}_3)$ fragment. The capped octahedral cluster on the right of the Figure is the more stable because the arrangement of ligands induces a greater hybridisation of Au 6s character into the $1a_1$ and $2a_1$ cluster bonding MOs illustrated.

TABLE 1
RELATIVE ENERGIES OF SOME PENTANUCLEAR GOLD CLUSTERS

Geometry	$\text{Au}_7(\text{PH}_3)_7^{3+}$	$\text{Au}_7(\text{PH}_3)_7^+$	$\text{Au}_7(\text{PH}_3)_7^-$
Pentagonal bipyramid	0.0	0.0	0.0
Capped octahedron (8)	+0.2	-1.5	-0.4
Capped octahedron (10)	-0.9	+1.2	-0.7

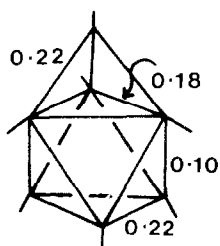
As a consequence of this reduction in symmetry there is a localisation of the P^σ contribution to the t_{1u} set in the $2a_1$ component accounting for its stabilisation whilst the $1e$ set acquires greater P^π character and is therefore destabilised. Introduction of a capping $\text{Au}(\text{PH}_3)$ fragment gives **10** which has a similar spectrum of MOs to that for **8**, see Fig. 3.



(10)

The relative energies of $\text{Au}_7(\text{PH}_3)_7$ with the different charges and geometries are summarised in Table 1.

These energies confirm that for $\text{Au}_7(\text{PH}_3)_7^{3+}$ the large stabilisation of $2a_1$ in **10** compared with **8** lead to the former being the most stable species.



(11)

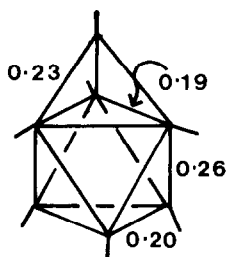
The overlap populations are reproduced in **11**, and reflect the fact that $2a_1$ is antibonding between the two triangular faces perpendicular to the C_3 axis. In the case of $\text{Au}_7(\text{PH}_3)_7$, **10** is still preferred over **8**, although the margin is smaller because the $1e$ set is less strongly bonding in the former.

TABLE 2a
PARAMETERS FOR NON-METAL ATOMS

Atom	Orbital	Slater Exponent	H_{ii} (eV)	Reference
H	1s	1.30	-13.60	17
P	3s	1.60	-18.60	18
	3p	1.60	-14.00	18

TABLE 2b
PARAMETERS FOR GOLD ATOM

Orbital	H_{ii} (eV)	ξ_1	c_1	ξ_2	c_2	Reference
6s	-9.22	2.60				19
6p	-4.27	2.58				19
5d	-11.85	6.16	0.648	2.73	0.539	19



(12)

The overlap populations for the former species, reproduced in **12**, are much more symmetrical than in the case of **11** since the 1e set is bonding between the two triangular faces perpendicular to the C_3 axis.

In conclusion therefore although the pentagonal bipyramidal $\text{Au}_7(\text{PR}_3)_7^+$ can be rationalised in terms of the MO arguments presented here, the clusters $\text{Au}_7(\text{PR}_3)_7^{3+}$ or $\text{Au}_6\text{Hg}(\text{PR}_3)_7$ are predicted to have capped octahedral geometries.

Appendix

All the calculations were performed using the Extended Hückel method with the relevant orbital parameters given in Tables 2a and 2b.

All the parameters conform to those which have been used to give reliable conclusions for organo-transition metal compounds [20]. The off-diagonal terms in the Extended Hückel calculations were estimated from the expression $H_{ij} = 1.75 S_{ij} (H_{ii} + H_{jj})/2$ [21].

The following bond lengths were used for the calculations: Au-Au 2.70 Å; Au-P 2.27 Å; P-H 1.42 Å. The calculations were performed on the ICL 2988 Computer at this University using the programs ICON8 and FMO [22].

Conclusions

Although there is a close analogy between the total number and symmetries of the molecular orbitals of B_nH_n and $Au_n(PR_3)_n$ clusters, the number of bonding MOs available for occupation is much larger in the former case. In the case of gold the poor overlap between gold $6p$ orbitals together with their high-lying nature militates against the occupation of any MO with predominantly Au $6p$ character. In general the gold clusters adopt the metal core and ligand conformation which leads to the maximum hybridisation of Au $6s$ character into the cluster bonding MOs. The general principles developed here have been used to predict the stoichiometry and geometrical features of a number of, as yet unknown, homo- and hetero-nuclear clusters containing gold.

Acknowledgements

The S.E.R.C. is thanked for financial support.

References

- 1 C.E. Briant, K.P. Hall and D.M.P. Mingos, *J. Organomet. Chem.*, 254 (1983) C18.
- 2 W. Bos, J.J. Bour, J.W.A. van der Velden, J.J. Steggarda, A.L. Cassalnuovo and L.H. Pignolet, *J. Organomet. Chem.*, 253 (1983) C64.
- 3 K.P. Hall and D.M.P. Mingos, *Prog. Inorg. Chem.*, 32 (1984) 237.
- 4 D.M.P. Mingos, *J. Chem. Soc., Dalton Trans.*, (1976) 1163.
- 5 C.E. Briant, B.R.C. Theobald, J.W. White, L.K. Bell, A.J. Welch and D.M.P. Mingos, *J. Chem. Soc., Chem. Commun.*, (1981) 201.
- 6 D.G. Evans and D.M.P. Mingos, *J. Organomet. Chem.*, 232 (1982) 171.
- 7 K.P. Hall, D.I. Gilmour and D.M.P. Mingos, *J. Organomet. Chem.*, 268 (1984) 275.
- 8 J.W.A. van der Velden, P.T. Beurskens, J.J. Bour, W.P. Bosman, J.H. Noordik, M. Kolenbrander and J.A.K.M. Buskes, *Inorg. Chem.*, 23 (1984) 146.
- 9 A.J. Stone, *Inorg. Chem.*, 20 (1981) 563.
- 10 A.J. Stone, *Molecular Physics*, 41 (1980) 1339.
- 11 K.P. Hall, B.R.C. Theobald, D.I. Gilmour, D.M.P. Mingos and A.J. Welch, *J. Chem. Soc., Chem. Commun.*, (1982) 528.
- 12 D.H. Farrar, B.F.G. Johnson, J. Lewis, J.N. Nicholls, P.R. Raithby and M.J. Rosales, *J. Chem. Soc. Chem. Commun.*, (1981) 273.
- 13 G. Longoni, M. Manassero and M. Sansoni, *J. Amer. Chem. Soc.*, 192 (1980) 3242.
- 14 D.G. Evans and D.M.P. Mingos, *Organometallics*, 2 (1983) 435.
- 15 B.F.G. Johnson, D.A. Kaner, J. Lewis and P.R. Raithby, *J. Chem. Soc., Chem. Commun.*, (1981) 753.
- 16 J.W.A. van der Velden and Z.M. Stadnik, *Inorg. Chem.*, 23 (1984) 2640.
- 17 R. Hoffman, *J. Chem. Phys.*, 39 (1963) 1397.
- 18 E. Clementi, *J. Chem. Phys.*, 40 (1964) 1944.
- 19 F.A. Cotton and C.B. Harris, *Inorg. Chem.*, 6 (1967) 369.
- 20 R. Hoffmann, *Science*, 211 (1981) 995 and refs. therein.
- 21 R. Hoffmann and W.N. Lipscomb, *J. Chem. Phys.*, 36 (1962) 2179.
- 22 J. Howell, A. Rossi, D. Wallace, K. Haraki and R. Hoffmann, *Quantum Chemistry Program Exchange*, 10 (1977) 344.